DOI: 10.1002/ ((please add manuscript number))
Article type: Full Paper

Off/on fluorescent nanoparticles for tunable high-temperature threshold sensing

*Alex Julià-López, Daniel Ruiz-Molina, Katharina Landfester, Markus B. Bannwarth, Claudio Roscini**

A. Julià-López, Dr. D. Ruiz-Molina, Dr. C. Roscini
Catalan Institute of Nanoscience and Nanotechnology (ICN2), CSIC and The Barcelona Institute of Science and Technology (BIST), Campus UAB, Bellaterra, 08193, Barcelona, Spain.
E-mail: Claudio.roscini@icn2.cat
Prof. Katharina Landfester, Dr. Markus B. Bannwarth
Max Planck Institute for Polymer Research, Ackermannweg 10, 55128 Mainz, Germany

Keywords: threshold-temperature sensors, polymeric nanoparticles, fluorescence enhancement, aggregation caused quenching, disaggregation induced emission

Abstract. Herein we report a versatile threshold temperature sensor based on the glass transition temperature-triggered fluorescence activation of a dye/developer duo, encapsulated in polymeric nanoparticles. The emission enhancement, detectable even by naked-eye is completed within a narrow temperature range and activates at adjustable threshold temperatures up to 200 ºC. Fluorescence was chosen as sensing probe due to its high detection sensitivity together with an advanced spatial and temporal resolution. The strategy is based on nanoparticles prepared from standard thermoplastic polymers, a fluorescence developer and the commercially available Rhodamine B base dye, a well-known and widely used fluorescent molecule. By making nanoparticles of different thermoplastic polymers, we were able to achieve fast, abrupt and irreversible disaggregation induced fluorescence enhancement, with tunable threshold temperature depending on the nanoparticles polymer glass transition. As a proof-of-concept for the versatility of this novel family of NPs, we show their use for sensing the thermal history of environments and surfaces exposed to the threshold temperature.

1. Introduction

Temperature tunable chromogenic and/or emissive sensors have been proposed during the last decades as a fast, easy and reliable way to measure[1] and/or indicate instantaneous temperature changes (reversible systems) or thermal histories (irreversible systems), without the need of intrusive and cost expensive techniques.[2] These emerging materials can be used in a wide range of applications, from smart food packaging[1b] to fluorescent thermometers[3] or temperature indicators.[4,5] Still, to widen the choice of practical applications, it is imperative to find first simpler, more robust and general synthetic alternatives that permit their full execution, and then to implement them in novel areas of interest, mainly high temperature sensing, to monitor electronic components, measure thermal exposure of vehicle parts or as indicator in sterilization processes, among many other applications.[1,2,4] Therefore, the straightforward fabrication of a universal and robust temperature sensor based on molecular materials, with permanent, abrupt, well-defined optical variations (*e.g.* off/on fluorescence) and adaptable for sensing far above RT, represents nowadays a scientific and technological challenge.

One of the most fruitful approaches so far to obtain such sensors consists in the development of polymeric temperature tunable chromogenic materials.[2] In these systems, the temperature induced optical variations (color change or fluorescence activation/quenching) arise from changes in the polarity[6] and/or viscosity[7] of the dye containing polymeric matrix, which in turn triggers differential polymer-dye interactions[2,8] (proton transfer, hydrogen-bondings). Though successful, sensing materials based on this approach require specific chemical functionalities in the polymer and/or dye, one of the key limitations for their continuous implementation. Alternatively, glass-transition temperature (T_g) induced viscosity changes can also promote different aggregation states (excimers/aggregates,[9] charge transfer complexes[10]) of the dye molecules.[1,2,4,11] Such temperature-triggered dye aggregation uses

the tendency of aromatic molecules kinetically trapped within a matrix in the disaggregated state, to yield the thermodynamically favored aggregates once the T_g is reached. This is a more polymer independent approach that produces an irreversible color switch or luminescence activation/quenching and is generally exploited to provide optical sensors that are able to record the thermal history of a surface or environment.[9-11] However this strategy also suffers of drawbacks, such as the tiny and/or linear optical shifts (of mixed monomer/aggregate absorption),[4, 9c] the requirement of opportunely designed and synthesized dyes (e.g. cyano-oligo p-phenylene vinylene)[1, 2, 4] and the thermodynamic tendency to yield stable aggregates already at room temperature (RT) with time.[12] Moreover, though many examples of T_g-triggered irreversible temperature indicators operating around RT[13] or slightly above 100 ºC[14] have been reported, only a few examples can be found for high threshold-temperature sensors (≥ 130 °C).[4]

In a recent work, Klymchenko *et al.* reported polymeric nanoparticles containing Rhodamine B octadecyl derivatives whose fluorescence can be fine-tuned by controlling their aggregation state.[15] At high dye loads and with the use of small counterions, a non-fluorescent material is obtained due to the aggregation-caused quenching (ACQ)[16] of the Rhodamine B cationic dye. Nevertheless, dilution of the dye and/or use of bulkier counter-anions that favor disaggregation, provide bright and emissive NPs.[15] Herein we hypothesize that such static interconversion (so far induced only upon specific synthetic conditions) can be converted into a dynamic interconversion between the non-emitting (aggregated) and emitting (disaggregated) states of the parent non-protonated Rhodamine B base, upon a temperature increase above the T_g of the hosting polymer. Once in the glassy state, the Rhodamine (RhB) dye molecules may start diffusing, as observed during an extrusion process, disaggregating and triggering an abrupt emission enhancement. If successful and the disaggregated state remains kinetically trapped upon cooling the material back to RT, we should be able to establish a good off/on irreversible temperature sensing platform up to really high

temperatures with the use of a commercial dye and a simple fine-tune temperature control based on the polymer T_g.

2. Results and discussion

2.1. Synthesis of RhB@polymer NPs

To explore the viability of our approach, highly RhB-loaded polymer nanoparticles (2 wt.%) were prepared through the reaction-free emulsion–solvent evaporation method[18] (for more details see experimental section and **Scheme S1** in Supporting Information) by using as encapsulating matrix polystyrene (PS, T_g = 100 ºC),[17] a standard commercially available polymeric material. SEM (**Figure 1a**) corroborated the formation of the RhB@PS nanoparticles (80-150 nm) whereas a preliminary naked-eye inspection showed a visible pink color. The absorption (**Figure S1**) in the visible region (λ_{max} = 557 nm) confirmed the encapsulation of the dye on its coloured zwitterionic RhB-zw form (**Scheme S2**). This form is stabilized in the presence of polar protic or chlorinated solvents such as those used in the present synthesis, whereas the colourless (λ_{max}^{abs} = 316 nm)[19] and weakly-fluorescent lactone form (**Scheme S2**) is generally stabilized in non-polar solvents (*e.g.* cyclohexane).[19, 20] Worth to mention though, the Vis absorption band at (λ_{max} = 557 nm) is shifted by comparison with the one obtained for a bulk solution measurement (λ_{max}^{abs} = 545 nm)[19, 21] pointing out already to the formation of aggregates within the nanoparticles. This aggregation was confirmed by fluorescence spectra (**Figure 1b**), which exhibits a very weak and broad band at λ_{max} = 610 nm (~40 nm red-shifted with respect to the corresponding measurement in an organic solution). Both, the small intensity and the red-shift are characteristic for non-emitting RhB-zw aggregated states. For comparison purposes, we have also synthesized the same NPs but with a 5-fold RhB concentration decrease (0.4 wt.%), which favored: *a)* a narrower visible absorption band (λ_{max}^{abs} = 557 nm, **Figure S1a**) with a less intense shoulder at 518 nm (in line with the decrease of non-fluorescent aggregates)[15, 21b] and *b)* the observation of a ~7 times

more intense band, narrower and slightly blue-shifted (λ_{max} = 604 nm) fluorescence (**Figures 1b and S2**). These results evidenced the lack of aggregates at lower dye concentrations.

Once determining the minimum RhB concentration at which ACQ is produced for the PS NPs we obtained RhB-containing NPs with polymers of different nature and, therefore, different T_gs. Poly(methyl methacrylate) (PMMA, T_g = 105 ºC)[17] and poly(bisphenol A carbonate) (PC, T_g = 150 ºC)[17] were selected as they are standard commercially available polymers that allow for straightforward syntheses of NPs. Polyethersulphone (PES) and polyetherimide (PEI), engineering polymers with very high T_g (180 ºC[22] and 215 ºC,[22] respectively), were chosen because they could provide higher sensing temperatures. In all the cases, RhB@PMMA, RhB@PC, RhB@PES and RhB@PEI NPs could be successfully obtained (80-200 nm, **Figures S3**) with the same method as described above, with the exception of PEI, for which $CHCl_3$ was used to ensure a proper dissolution of the polymer. All NPs (dye content 2 wt. %) were pink coloured (*i.e.* RhB was encapsulated in its RhB-zw form) and not fluorescent (*i.e.* dye molecules were aggregated), as previously found for the PS nanoparticles.

-Insert Figure 1 here-

2.2. Temperature-dependence of RhB@polymer NPs

RhB@PS NPs were first heated for 10 min at increasing selected temperatures (70-105 ºC, see supporting information) and, after cooling down to RT, their fluorescence was measured by emission spectroscopy. The fluorescence spectra of the RhB@PS NPs heated from 25 ^{o}C to 105 ºC showed *i)* a progressive fluorescence enhancement ΔF,[23] defined as ΔF (T) = (F_T-F_{RT})/F_{RT}, up to ΔF^{max} = 47% (corresponding to the maximum enhancement, obtained at 105 ºC) and *ii)* the emission remains also after cooling (**Figures 1c-1d**). Such enhancement has been attributed to dye disaggregation processes upon softening and increased motion of the polymeric chains around the reported polystyrene T_g (100 ^{o}C).[17] In fact, the softening of the

polymer is clearly demonstrated by the complete loss of the NPs shape once this temperature is reached (**Figure S3a**). Moreover, the concomitant presence of other processes accounting for this temperature induced fluorescence increase was discarded. Indeed, enhancement of the RhB fluorescence quantum yield with temperature was excluded as it generally follows the opposite trend.[24] On the other side, the simultaneous existence of an equilibrium shift from the non-fluorescent lactone (colorless) to the emitting zwitterionic (colored) isomer was also left out as the latter is the original form already trapped along the formation of the NPs (accounting for their pink color). Similar behavior was found for the other families of NPs. Measurements done upon heating the NPs showed maximum fluorescence enhancements ΔF^{max} of 194% (at 120 ºC), 68% (140 ºC), 132% (160 ºC) and 292% (210 ºC) for RhB@PMMA, RhB@PC, RhB@PES and RhB@PEI NPs, respectively (**Figures 1d, S4**), with transition temperatures strongly correlated with the nature of the polymer (**Table S1**). In all cases, the observation at SEM of the NPs heated at the respective ΔF^{max} temperatures showed the loss of the NPs structure, indicating that the complete enhancement is achieved upon reaching the NPs polymer T_gs (**Figure S3**).

These experiments confirmed our initial hypothesis, though the results were still far from ideal. Indeed, the fluorescence enhancement was not as high as desired (*e.g.* $\Delta F^{max\_RhB@PC}$ = 68%) and most of the times gradual (**Figure 1d**), making these NPs not ideal to develop precise off/on threshold sensors. Only RhB@PEI NPs (ΔF^{max}=292%) exhibited the complete off/on fluorescence switch within just 20 ºC. This was ascribed to: *i)* the high rigidity of PEI, which does not allow the dye molecules to diffuse until the polymer reaches its T_g and *ii)* the higher temperature needed to reach the T_g, which in turn tips the system with more energy to efficiently disaggregate the dyes. To overcome this limitation, we proposed the co-encapsulation of additives favoring the diffusion and the disaggregation of RhB at higher temperatures. As a candidate we considered dodecanoic acid (DA), a twelve-carbon non-

volatile weak acid with melting point (T_m) of 43.8 ºC.[25] The reason for this choice is threefold. Above its T_m, DA is expected to act as *a)* plasticizer of the polymer, increasing the RhB molecules mobility, *b)* intercalate between the RhB molecules through the formation of H-bonding and *c)* it is also known to form complexes with spirolactones and spiropyrans molecules through H-bonding interactions, inducing the opening to the colored and/or fluorescent form.[5]

2.3. Synthesis of RhB/DA@polymer NPs sensors

Before any nanostructuration, the DA-RhB interaction was initially investigated in bulk solutions, both in solid ($T < T_m^{DA}$) and liquid state ($T > T_m^{DA}$). The pink and highly fluorescent (λ_{max}^{emi} = 595 nm) solution obtained by dissolving the RhB-base in liquid DA ($T > T_m^{DA}$, 47 μM) was in agreement with the formation mostly of the RhB-zw form (**Figure S5**). The lack of any fluorescence enhancement upon addition of glacial acetic acid (**Figure S6**), which is described to boost the formation of the RhB-zw form,[20, 21a] confirmed that the formation of this species was almost quantitative already in liquid DA. At lower temperatures ($T < T_m^{DA}$), the solution solidified while maintaining the pink color characteristic of the RhB-zw form. However, in this case, the fluorescence was almost completely quenched (λ_{max}^{emi} = 627 nm) most likely due to the formation of the insoluble aggregates (**Figure S5**). These results confirmed the influence of DA on the aggregation-caused fluorescence quenching.

Again, the optimization of the synthesis of DA-containing nanoparticles was carried out using PS as matrix (RhB/DA@PS) and following the same methodology used for RhB@PS nanoparticles (2 wt.% RhB respect to PS), but adding now DA (10 wt.% respect to PS) to the mixture, just before the emulsification process (see Experimental Section, **Scheme S1**). Such addition resulted in an immediate color enhancement due to the DA-induced equilibrium displacement towards the non-aggregated RhB-zw form, and therefore, on a remarkable increase of the fluorescence solution (**Figure S7**). As expected, this was not the case upon dye

encapsulation in the polymer. The formation of the RhB/DA@PS NPs (120–200 nm) was corroborated by SEM (**Figure 2a**), whereas the encapsulation of DA was quantitatively confirmed (9 wt.%) through ^{1}H-NMR spectroscopy (**Figures S8**). The pink NPs showed only residual fluorescence (λ_{max}^{emi} = 622 nm) due to a large presence of aggregates of RhB-zw molecules (**Figure 2b-2d**). Once more, the influence of the aggregation state on the emission properties of the nanoparticles was confirmed upon decreasing (diluting) the percentage of the dye (0.4 wt.% of RhB with respect to PS). In this case, a much more intense (**Figures S9a and S9c**) and narrower (**Figures S9b**) fluorescence emission (λ_{max}^{emi} = 605 nm) was found at room temperature.

- Insert Figure 2 here -

RhB/DA@PMMA, RhB/DA@PC, RhB/DA@PES and RhB/DA@PEI NPs (2 wt.% RhB) were thus obtained following a similar methodology. SEM images (**Figure S10**) and ^{1}H-NMR (**Figures S11-S14**) confirmed in all cases the formation of nanoparticles (80-200 nm) with good DA encapsulation yields (8.6, 7.4, 8.7, 9.0 wt.%, respectively). Notably, despite the well-known costs and difficulties for the PES and PEI processability in standard extrusion/injection molding processes, the highly loaded non-fluorescent RhB/DA@PES and RhB/DA@PEI NPs were very easy to achieve through a scalable method. All NPs were pink colored and showed only a little fluorescence emission (λ_{max}^{PMMA} = 619 nm, λ_{max}^{PC} = 624 nm, λ_{max}^{PES} = 621 nm and λ_{max}^{PEI} = 623 nm), indicating again the encapsulation of RhB-zw molecules as non-emitting aggregates under these conditions (**Figure S15**). Finally, the DSC analysis of the NPs showed that DA plasticizes the polymers, inducing therefore changes in the measured T_g of the NPs polymer (93, 95, 100-150, 150 and 186 ºC), making them lower (in the case of PS, PMMA, PES and PEI NPs)[17, 22] or broader (PC)[17] than the reported

values for the corresponding plain bulk polymers (**Figure S16**). These are the temperatures around which the observation of the fluorescence enhancement is expected.

2.4. Temperature-dependence of RhB/DA@polymer NPs

Fluorescence spectra of RhB/DA@PS NPs were recorded at room temperature after heating the NPs for 10 min at increasing temperature within the 25 °C-110 °C range (see **Figures 2b-2c**). Between 25 °C and 70 °C, the fluorescence intensity remained practically constant (**Figures 2b-2c**) with a partial narrowing of the emission band (**Figure S17**), just above the melting point of the DA (43.8 ºC). Tangible indication for emission enhancement was observed above 80°C (ΔF = 69%) that became much more evident (ΔF = 231%) once the NPs were heated for 10 min at 90 °C (**Figure 2d**) and levels at its maximum value of 100-110 ºC (ΔF^{max} = 266%). First evidence of the positive effect of DA was the strongly enhanced fluorescence between the maximum emitting and non-emitting (ΔF^{max} = 266% obtained at 100-110 ºC) states in comparison to the corresponding NPs lacking DA (ΔF^{ma} = 47%, at 105 ºC), and was high enough as to be detectable even by naked eye (**Figures 2d** and **S18**). The increase of the fluorescence intensity, which was also irreversible, was accompanied by a little blue shift (from λ_{max} = 627 nm to 618 nm) and a further narrowing of the emission band (**Figure S17**). Finally, any chemical degradation of RhB into different and more fluorescent species that account for the emission enhancement was discarded by analyzing the negligible changes of the RhB absorption spectra before and after annealing in both the solid state and dissolved in $CHCl_3$ (**Figure S19**).

For comparison purposes, three additional color-developers were also tested: nonanoic acid (NA), tetradecanol (TD) or Miglyol®812 (a caprylic/capric triglyceride, M812). Worth to mention, only in the case of NA-doped NPs an evident off/on fluorescence enhancements (ΔF^{max} = 313%) was observed, most likely due to its similar chemical composition of DA and

its tendency to form hydrogen bonds (**Figure S20**). In contrast, TD (ΔF^{max} = 104%) and M812 (ΔF^{max} = 7.4%) induced a linear or no fluorescence increase.

Variable-temperature emission spectra of RhB/DA@PMMA, RhB/DA@PC, RhB/DA@PES NPs and RhB/DA@PEI NPs were finally studied and showed to exhibit the same leanings (Figures S22-S23):

a) no significant fluorescence changes were observed until 5-10 ºC below the corresponding measured polymer T_gs (95 ºC, 100-150 ºC, 150 ºC and 186 ºC respectively, **Figures S15-S16**).

b) The transition is fast (<10 min), once the T_g of the NPs polymer is reached (**Figures 2c**, **S15**, **S21** and **Table S1**), and far more abrupt - ΔF^{max} = 611% (120 ºC), 438% (130 ºC), 328% (160 ºC), 253% (200 ºC), respectively - than for the respective NPs lacking DA (the only exception is given by PEI, which gave similar enhancement features with and without DA), and accompanied by narrowing and blue-shifting of the bands (**Figure S22**). Notably, the maximum fluorescent enhancement (ΔF^{max}) is between 10 and 25 ºC above the measured T_g of the NPs polymer. This little discrepancy between the measured T_g of the NPs polymer and the threshold fluorescence activation, was ascribed to the different procedures and equipment used in both techniques.[26]

c) The fluorescence is retained upon cooling down to room temperature, where the spherical morphology of the initial nanoparticles is lost according to SEM images (**Figure S23**).

Moreover, the non-specificity of M812 as color developer in different NPs provides different results depending on the nature of the polymer: RhB/M812@PS NPs do not show any enhancement, RhB/M812@PMMA NPs (600%) and RhB/M812@PES NPs (618%) present a more gradual increase of fluorescence. (**Figure S24**). These results reaffirmed DA as a good color-developer of choice.

2.5. Tunable threshold temperature sensors

The glass transition dependency of the fluorescence activation permits the use of these RhB/DA@polymer NPs for the implementation of threshold temperature sensors. As proof-of-concept we choose RhB/DA@PMMA NPs (which gave the highest ΔF^{max}), layered on top of a thermally conductive aluminum bar, as threshold temperature sensor (**video S1**, **Figures 3a** and **S25**). A thermopar attached to the bar, close to the NPs position, allowed for the direct measurement of the surface temperature. When the bar is held between 70 and 80 ºC for four minutes no fluorescence changes are observed. On the contrary, the emission of the NPs clearly increases within a minute while the temperature reaches 120 ºC, with the fluorescence completely and irreversibly turned on already at 110 ºC. The fluorescence enhancement is clearly detectable by naked eye and maintains once the bar is cooled back to lower temperatures (e.g. 70 ºC).

Similarly, with nanoparticles of different polymers (and different T_gs) in our hand, we were able to prepare a multiple threshold fluorescent sensor with the scope to permanently detect the history of a surface or environment exposed to increasing temperatures (**Figure 3b**). In this case RhB/DA@PMMA, RhB/DA@PES and RhB/DA@PEI NPs were layered in three metal containers and simultaneously subjected (for 10 min) at increasing temperatures inside an oven. Thus, we were able to observe, by naked eye, selective fluorescence turning on upon temperature increase, with RhB/DA@PMMA activating first (T = 100 ºC), then RhB/DA@PES NPs (T = 140 ºC) and finally RhB/DA@PEI NPs (T = 200 ºC).

As far as we know, this is the first RhB-based solid fluorescence thermometer revealing threshold temperatures as high as 200 ºC. Previously described RhB@polymer thermometers were reversible, working exclusively in a selective range of temperatures and did require the integration of the dye through chemical modifications and syntheses.[6b, 6c]

- **Insert Figure 3 here –**

3. Conclusion

In summary, in this work we report a novel, general and straightforward methodology for the development of fluorescent tunable threshold temperature sensors able to record the thermal history of surfaces and environments over a broad range of temperatures, from 90 up to almost 200 °C, unusually high for a molecular-based sensor. The strategy is based on the encapsulation of Rhodamine B base together with a developer within polymeric NPs, easily prepared from commercially available polymers and without requiring additional design and/or synthesis of new molecular dyes. The NPs provide *a)* abrupt (30 ºC) and fast (<10 min) fluorescence enhancements around the glass transition temperature due to the developer-induced disaggregation of RhB molecules within the polymer, *b)* easy tunability of the threshold fluorescence activation temperature by simply changing the constituent polymer and *c)* an irreversible cooled down (to room temperature) fluorescing sensing material that allows recording the thermal history of surfaces and/or environments exposed to overheating. Interestingly, the fluorescence appearance from the polymeric NPs can be detected by naked eye without the need of any auxiliary equipment and can be easily adapted to any thermoplastic polymer, copolymer and blend suitable for NPs synthesis. This also includes scarcely reported very high temperatures (140-200 °C) sensing systems based on molecular materials and easily prepared NPs made by high T_g polymers which are normally costly and difficult to process in conventional ways. Moreover, the developed aqueous colloidal dispersion of the thermochromic NPs can be easily applied onto various materials allowing for a wide range of sensing applications that require irreversible high-temperature detection.

4. Experimental Section

See supporting information for the experimental section.

Supporting Information

Supporting Information is available from the Wiley Online Library or from the author.

Acknowledgements
This work was supported by project MAT2015-70615-R from the Spanish Government and by FEDER funds and by the Max Planck Society. ICN2 acknowledges support from the Severo Ochoa Program (MINECO, Grant SEV-2013-0295). Funded by the CERCA Programme/Generalitat de Catalunya.

Received: ((will be filled in by the editorial staff))
Revised: ((will be filled in by the editorial staff))
Published online: ((will be filled in by the editorial staff))

References

[1] *a)* B. R. Crenshaw, C. Weder, *Adv. Mater.* **2005**, *17*, 1471-1476; *b) Food Process Modelling*, (Eds: L. M. M. Tijskens, M. L. A. T. M. Hertog, B. M. Nicolaï Woodhead Publishing Limited, Cambridge, UK, **2001**, chapt. 19.

[2] A. Seeboth, D. Lötzsch, R. Ruhmann, O. Muehling, *Chem. Rev.* **2014**, *114*, 3037-3068.

[3] J. Feng, L. Xiong, S. Wang, S. Li, Y. Li, G. Yang, *Adv. Funct. Mater.* **2013**, *23*, 340–345.

[4] C. E. Sing, J. Kunzelman, C. Weder, *J. Mater. Chem.*, **2009**, *19*, 104–110.

[5] *a)* M. A. White, M. LeBlanc, *J. Chem. Educ.* **1999**, *76,* 1201-1204; *b)* F. Azizian, A. J. Field, M. Heron, C. Kilner, *Chem. Commun*. **2012**,*48*, 750–752; *c)* F. Azizian, A. J. Field, M. Heron, *Dyes Pigm.* **2013**, 99, 432-439.

[6] *a)* S. Uchiyama, Y. Matsumura, A. P. De Silva, K. Iwai, *Anal. Chem.* **2003**, *75*, 5926-5935; *b)* Y. Shiraishi, R. Miyamoto, X. Zhang, T. Hirai, *Org. Lett.* **2007**, *9*, 3921-3924; *c)* Y. Shiraishi, R. Miyamoto, T. Hirai, *J. Photochem. Photobio. A* **2008**, *200,* 432–437; *d)* F. Donati, A. Pucci, G. Ruggeri, *Phys. Chem. Chem. Phys.* **2009**, *11*, 6276-6282.

[7] C. C. White, K. B. Migler, W. L. Wu, *Polym. Eng. Sci.* **2001**, *41*, 1497-1505.

[8] A. Seeboth, D. Lötzsch, R. Ruhmann, *J. Mat. Chem. C* **2013**, *1*, 2811-2816.

[9] *a)* J. B. Birks in *Photophysics of Aromatic Molecules,* Wiley-Interscience, London, New York, **1970**; *b)* C. J. Ellison, J. M. Torkelson, *J. Polym. Sci., Part B: Polym. Phys.* **2002**, *40*, 2745–2758, *c)* O. van den Berg, W. G. F. Sengers, W. F. Jager, S. J. Picken, M. Wübbenhorst, *Macromolecules* **2004**, *37*, 2460-2470; *d)* B.-S. Lee, H.S. Shin, *Food Sci. Biotechnol.* **2012**, *21*, 1483-1487.

[10] T. Corrales, C. Abrís i, C. Peinado, F. Catalina, *Macromolecules* **2004**, *37*, 6596-6605.

[11] S.-h. Guo, F.-y. Zheng, F. Zeng, S.-z. Wu, *Chin. J. of Polym. Sci.* **2016**, 34, 830-837.

[12] A. Pucci, F. Signori, R. Bizzarri, S. Bronco, G. Ruggeri, F. Ciardelli, *J. Mat. Chem.* **2010**, *20*, 5843-5852.

[13] *a)* B. R. Crenshaw, J. Kunzelman, C. E. Sing, C. Ander, C. Weder, *Macromol. Chem. Phys.* **2007**, *208*, 572–580; *b)* C. Seiter, US Patent 4 057 029, **1977**; c*)* R. Arens, R. D. Birholz, D. L. Johnson, T. P. Labuza, C. L. Larson, D. J. Yarusso, US Patent 5 667 303, **1997**.

[14] *a)* M. Kinami, B. R. Crenshaw, C. Weder, *Chem. Mater.* **2006**, *18*, 946-955; *b)* J. Kunzelman, B. R. Crenshaw, M. Kinami, C. Weder, *Macromol. Rapid Commun.* **2006**, *27*, 1981–1987.

[15] *a)* A. Reisch, P. Didier, L. Richert, S. Oncul, Y. Arntz, Y. Mély, A. S. Klymchenko, *Nat. Comm.* **2014**, *5*, 4089; *b)* I. Shulov, S. Oncul, A. Reisch, Y. Arntz, M. Collot, Y. Mély, A. S. Klymchenko, *Nanoscale* **2015**, *7*, 18198-18210.

[16] *a)* Y. Hong, J. W. Y. Lama, B. Z. Tang, *Chem. Commun.* **2009**, 4332–4353; *b)* J. Mei , Y. Hong , J. W. Y. Lam , A. Qin , Y. Tang , B. Z. Tang, *Adv. Mater.* **2014**, *26*, 5429–5479; *c)* G. Feng, R. T. K. Kwok, B. Z. Tang, B. Liu, *Appl. Phys. Rev.* **2017**, *4*, 021307-1-41; *d)* J. Mei, N. L. C. Leung, R. T. K. Kwok, J. W. Y. Lam, B. Z. Tang, *Chem. Rev.* **2015**, *115*, 11718− 11940; *e)* H. Zhang, X. Zheng, Ni X., Z. He, J. Liu, N.

L. C. Leung, Y. Niu, X. Huang, K. S. Wong, R. T. K. Kwok, H. H. Y. Sung, I. D. Williams, A. Qin, J. W. Y. Lam, B. Z. Tang, *J. Am. Chem. Soc.* **2017**, *139*, 16264-16272; *f)* X. Ma, R. Sun, J. Cheng, J. Liu, F. Gou, H. Xiang, X. Zhou, *J. Chem. Educ.* **2016**, *93*, 345–350; *g)* W. Z. Yuan, P Lu, S. Chen, J. W. Lam, Z. Wang, Y. Liu, H. S. Kwok, Y. Ma, B. Z. Tang, *Adv. Mater.* **2010**, *22*, 2159-2163.

[17] J. E. Mark ed., in *Polymer data Handbook*; Oxford University Press, **1999**.

[18] *a)* Y. Zhao, J. Fickert, K. Landfester , D. Crespy, *Small* **2012**, *8*, 2954–2958; b) R. H. Staff , D. Schaeffel , A. Turshatov , D. Donadio, H.-J. Butt , K. Landfester , K. Koynov, D. Crespy, *Small* **2013**, *9*, 3514–3522; *c)* M. Hu, S. Peil, Y. Xing, D. Döhler, L. C. da Silva, W. H. Binder, M. Kappla, M. B. Bannwarth, *Mater. Horiz.*, **2018**, *5*, 51-58.

[19] U. K. A. Klein, F. W. Hafner, *Chem. Phys. Lett.* **1976**, *43,* 141-145.

[20] I. Rosenthal, P. Peretz, K. A. Muszkat, *J. Phys. Chem.* **1979**, *83,* 350-353.

[21] *a)* J.'H. Muto, *J. Phys. Chem.* **1976**, *80*, 1342-1346; *b)* J. L. Dela Cruz, G. J. Blanchard, *J. Phys. Chem. A* **2002,** *106*, 10718-10724.

[22] C. L. Harper, E. M. Petrie in *Plastic Materials and Processes: A concise Encyclopedia*, Wiley & Sons, Inc., **2003**.

[23] The emission enhancement at a given temperature $\Delta F(T)$ was calculated from the equation $(F_T-F_{RT})/F_{RT}$, where F_T and F_{RT} are the integrated emission intensities obtained from the RhB emission bands after heating the NPs at the specific temperature T and at RT, respectively. ΔF^{max} is the maximum enhancement obtained for the heated NPs.

[24] R. F. Kubin, A. N. Fletcher, *J. Lumin.* **1982**, *27,* 455-462.

[25] J. R. Rumble, ed., *CRC Handbook of Chemistry and Physics*, Internet Version, CRC Press, Boca Raton, FL, **2005** http://www.hbcpnetbase.com (accessed February 23, 2018).

[26] While in DSC the NPs were heat at 10°C/min in a closed aluminum sample holder, in fluorescence experiments the NPs were heat at a set temperature in a glass vial for 10 min.

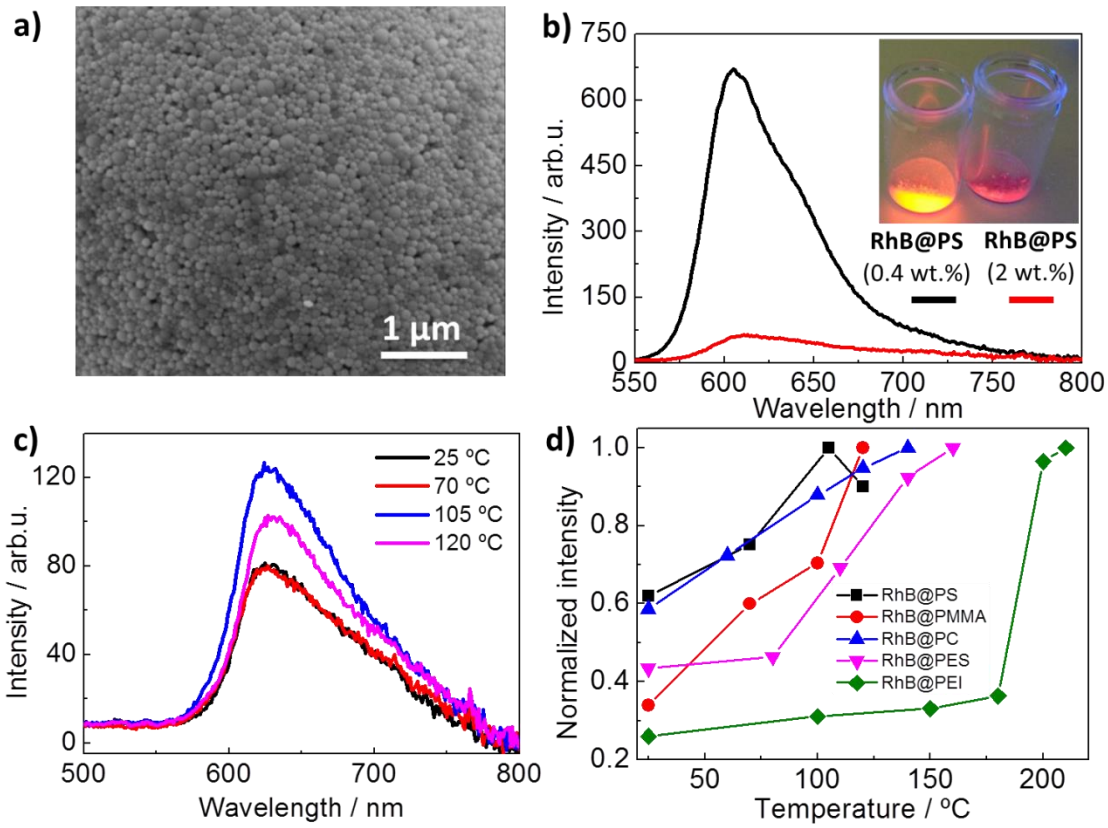

Figure 1: Morphology and fluorescent properties of polymer NPs containing RhB. *a)* SEM image of the RhB@PS NPs; *b)* fluorescence spectra (λ_{exc}= 355 nm) and digital photos (inset) in presence of UV light (λ_{exc}=365 nm) of the RhB@PS NPs with two different RhB concentrations (2 wt. % and 0.4 wt. %); *c)* fluorescence emission spectra (λ_{exc} = 355 nm) of the RhB@PS NPs (2 wt.%), recorded at RT, after heating the NPs at different temperatures; *d)* integrated emission intensities (normalized respect to the most intense spectrum obtained from each series) of the NPs *vs* temperature.

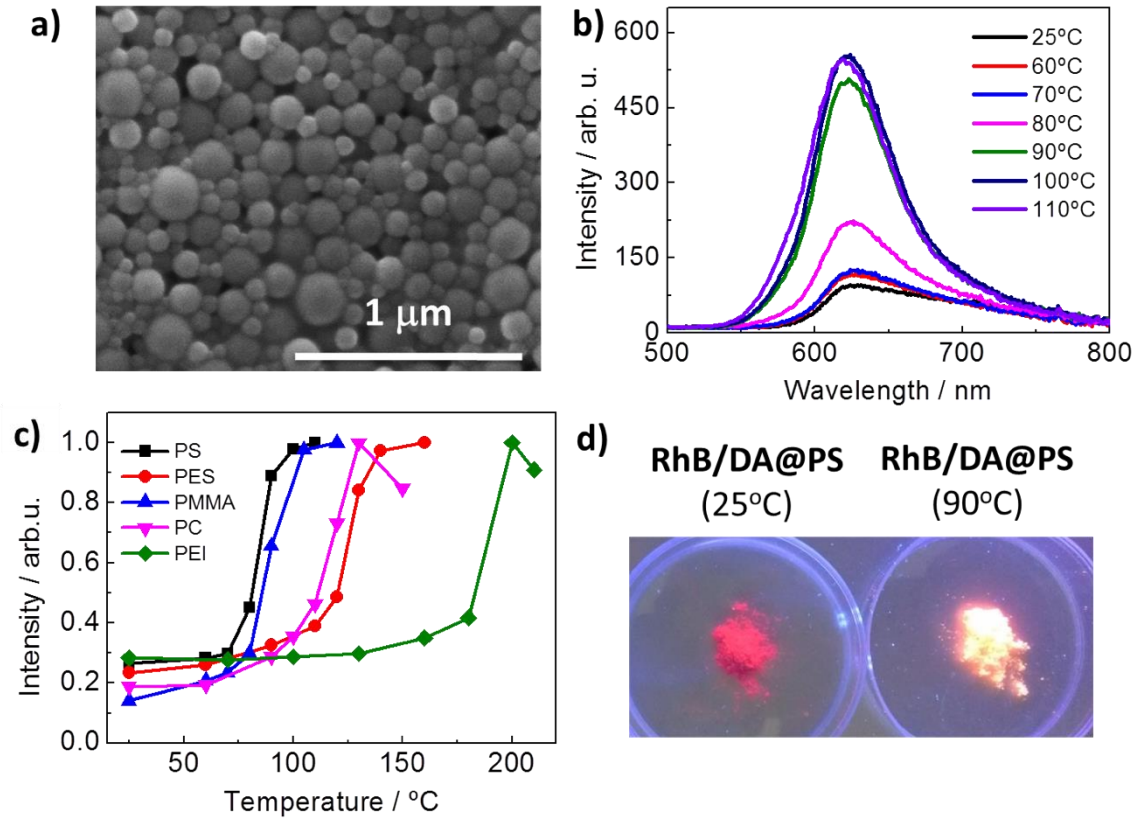

Figure 2: Morphology and fluorescent properties of polymer NPs containing RhB and DA. *a)* SEM image of RhB/DA@PS NPs; *b)* emission spectra (λ_{exc} = 355 nm) of the RhB/DA@PS nanoparticles (2 wt.%), recorded at RT after heating the NPs at different temperatures; *c)* integrated emission intensities of RhB/DA containing NPs made of different polymers (normalized to the most intense spectrum) *vs* temperature; *d)* digital photographs of RhB/DA@PS at 20°C and above 90°C, under UV light (λ_{exc} = 365 nm);

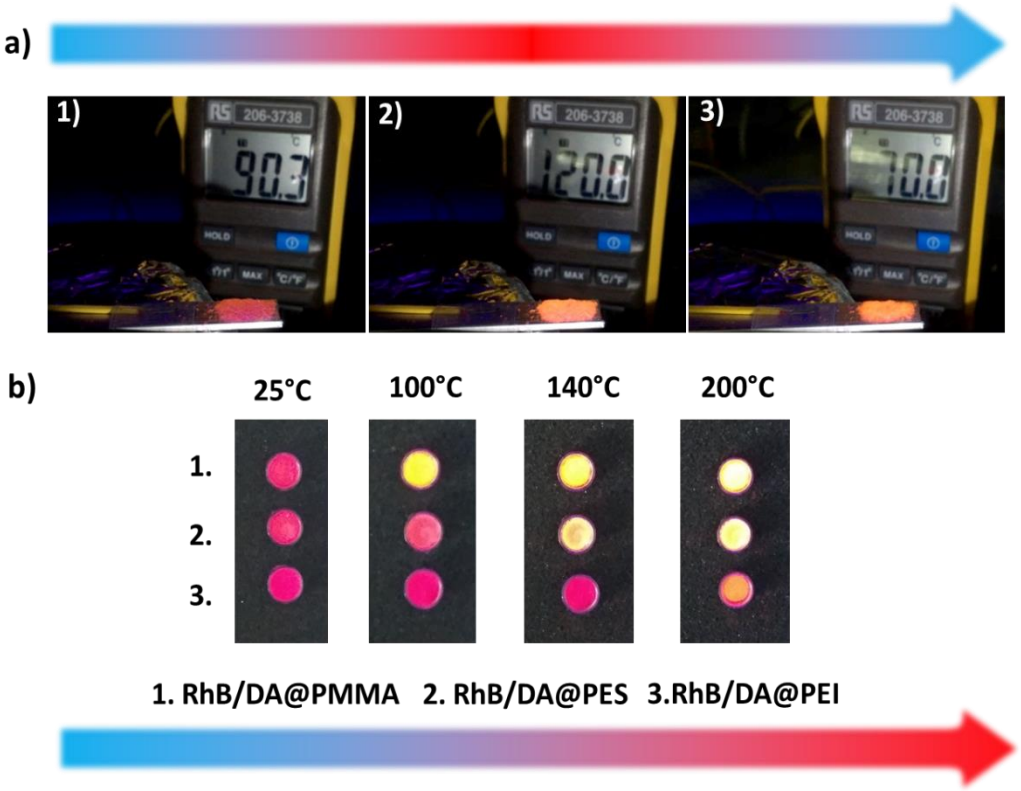

Figure 3. *a)* Snapshots of the video S1 (see supporting information) showing the fluorescence enhancement between 90 and 125 ºC and the fluorescence maintenance once back to lower temperatures (λ_{exc} = 365 nm); *b)* digital photos of the RhB/DA@PMMA, RhB/DA@PC and RhB/DA@PES NPs in aluminum containers after being exposed to different temperatures (λ_{exc} = 365 nm).

Fluorescent high-temperature threshold sensors, based on polymeric nanoparticles containing Rhodamine B and dodecanoic acid, are obtained. These sensors are easily prepared to selectively detect threshold temperatures in the range of 90-200 ºC, by simply changing the constituent polymer. The irreversible fluorescence enhancement is high enough to be detectable by naked-eye.

threshold-temperature sensors, polymeric nanoparticles, fluorescence enhancement, aggregation caused quenching, disaggregation induced emission

*A. Julià-López, D. Ruiz-Molina, K. Landfester, M. B. Bannwarth, C. Roscini**

Off/on fluorescent nanoparticles for tunable high-temperature threshold sensing